Table 5 (cont.)

Angles

C(6')–Mo—N(1)	98·92 (16)
C(6')–Mo—N(1')	105·33 (15)
N(1) –Mo—N(1')	80·87 (16)
N(1) –Mo—H1(B)	73·2
C(6)—Mo—H1(B)	98·9
B——N(2) –N(1)	113·72 (47)
B——N(2) –C(3)	136·24 (41)
B——N(2')-N(1')	114·21 (28)
B——N(2')-C(3')	134·53 (44)
N(2) –B——N(2')	107·90 (39)
N(1) –N(2) –C(3)	110·01 (26)
N(2) –C(3) –C(2)	107·08 (52)
C(3)—C(2)—C(1)	106·83 (33)
C(2)—C(1)—N(1)	108·78 (40)
C(1)—N(1) –N(2)	107·17 (25)
N(2) –C(3)—C(5)	121·67 (35)
C(2)—C(3)—C(5)	131·21 (42)
N(1) –C(1)—C(4)	121·14 (30)
C(2)—C(1)—C(4)	130·03 (45)
N(1')-N(2')-C(3')	110·80 (28)
N(2')-C(3')-C(2')	106·44 (52)
C(3')-C(2')-C(1')	106·86 (48)
C(2')-C(1')-N(1')	109·32 (31)
C(1')-N(1')-N(2')	106·59 (26)
N(2')-C(3')-C(5')	123·00 (32)
C(2')-C(3')-C(5')	130·59 (45)
N(1')-C(1')-C(4')	120·37 (33)
C(2')-C(1')-C(4')	130·78 (42)
C(7)—C(8)—C(9)	118·38 (36)

The allyl group is compelled by steric reasons to assume the position shown in Fig. 1. Very short contact distances from the two carbonyl groups (2·46–2·55 Å), as well as from one pyrazolyl group (3·07 Å), hinder rotation of the allyl group. For the same reason, the distances of C(7) and C(9) from Mo (2·33 and

2·36 Å) are considerably longer than the Mo–C(8) distance (2·21 Å).

As for the other geometrical parameters (Fig. 2), there are no remarkable differences between this and the similar compund hydrotris-(1-pyrazolyl)boratobenzenediazodicarbonylmolybdenum (Avitabile, Ganis & Nemiroff, 1970). Bond lengths and angles are quite normal. The greater distance Mo–N(1') (2·25 Å) with respect to Mo–N(1) (2·18 Å) can be due to the non-bonded interaction C(9)–N(1') and C(8)–N(1'), both about 3·07 Å.

Fig. 3 shows the packing of dihydro-(3,5-dimethyl-1-pyrazolyl)boratodicarbonylmolybdenum-π-allyl on [100]. The shortest intermolecular contact distances are reported.

We are indebted to Professor S. Holt, who suggested this project, Dr S. Trofimenko, who provided the compound and Professor G. Allegra, who aided in the collection of the data.

References

AVITABILE, G., GANIS, P. & NEMIROFF, M. (1971). Acta Cryst. B27, 725.
CHURCHILL, M., GOLD, K. & MAW, C. (1970). Inorg. Chem. 9, 1597.
IMMIRZI, A. (1967). Ric. Sci. 37, 743, 846, 850. (These references include Fourier, structure factor, and least-squares programs.)
MOORE, F. H. (1963). Acta Cryst. 16, 1169.
TROFIMENKO, S. (1967). J. Amer. Chem. Soc. 89, 3170.
TROFIMENKO, S. (1968). J. Amer. Chem. Soc. 90, 4754.
TROFIMENKO, S. (1969a). J. Amer. Chem. Soc. 91, 588.
TROFIMENKO, S. (1969b). J. Amer. Chem. Soc. 91, 3183.
TROFIMENKO, S. (1970). Inorg. Chem. 9, 2493.

The Crystal Structure of a Pyrrhotite (Fe₇S₈)

BY M. E. FLEET

Department of Geology, University of Western Ontario, London, Ontario, Canada

The structure of a pyrrhotite exhibiting a hexagonal ($a=2A$, $c=3C$) supercell has been determined from analysis of three-dimensional single-crystal intensity data. The symmetry of the structure is trigonal, space group $P3_1$; the hexagonal symmetry shown by single crystals possibly results from twinning, in which platy domains stacked normal to c are related by 180° rotations about c. The structure is composed of 12 subcell units stacked in three layers of four. The vacancies in the Fe sites are ordered, confined to alternate layers of Fe atoms normal to c. The distortions observed in the structure are analogous to those in the structure of troilite. Three Fe atoms in each Fe layer are displaced toward an enlarged tetrahedral site; the displacements from the ideal positions are 0·22 Å in both the vacancy layers and the full Fe layers.

Introduction

Pyrrhotites have the general composition $Fe_{1-x}S$. Below 370°C most pyrrhotites exhibit some degree of superstructure development; the B–8 (NiAs) type structure of the subcell was assigned by Alsen (1925). Compositions at, or near, stoichiometric FeS have the hexagonal troilite superstructure with $a=A\sqrt{3}$, $c=2C$, where

A and C are the parameters of the subcell. Pyrrhotites that are more Fe-deficient than 48·8 atomic per cent of Fe generally have hexagonal superstructures, many apparently belonging to the series $a=2A$, $c=nC$ (Fleet & MacRae, 1969). A monoclinic superstructure with $a=2A\sqrt{3}$, $b=2A$, $c=4C$, $\beta=90\cdot45°$, occurs at, and near the composition Fe_7S_8, for which it was proposed that the supercell contained ordered vacancies in alternate Fe layers normal to the c direction (Bertaut, 1952). However, quantitative intensity measurements were not made in this investigation, and no rigorous comparison of observed and calculated structure factors was attempted.

Experimental

The present study was made on a single crystal of synthetic pyrrhotite reported to have a hexagonal superstructure with $a=2A$, $c=3C$ (Fleet, 1968). Material was synthesized by heating a mixture of Fe sponge and S crystals, of composition 45·48 atomic per cent Fe, in an evacuated SiO_2 tube at 900 °C for 2 days, 500 °C for 3 days, and then quenching the charge in water. The product consisted of pyrrhotite and pyrite. The composition of the pyrrhotite, determined from the d_{102} spacing–composition relation (Toulmin & Barton, 1964), is 46·5 atomic per cent Fe, essentially Fe_7S_8. Lattice parameters are $a=6\cdot8673\pm0\cdot0009$, $c=17\cdot062\pm0\cdot002$ Å, and the apparent space group is $P6_222$ (or $P6_422$). A single crystal, tabular in form, of approximate dimensions 0·1 mm diameter and 0·1 mm thick and with a few poorly developed hexagonal bipyramid faces, was selected for the study.

X-ray intensity data were collected on an integrating Weissenberg camera using Zr-filtered Mo $K\alpha$ radiation ($\lambda=0\cdot7107$ Å) for the first three subcell levels of the a axis. Films at each level were exposed for 1, 2, 4 and 9 complete integration cycles, which provided sufficient overlap to scale the intensities within the levels. The films were measured with a Joyce–Loebel Autodensidata densitometer, using the digitized output for those peaks with relative intensity greater than 2% of the 206 reflexion, and the chart output for the weak peaks. Raw intensity data were corrected for Lorentz and polarization factors and for absorption ($\mu=128\cdot3$ cm^{-1}). The reduced intensity data were scaled between levels using empirical factors calculated from equivalent reflexions; a total of 167 subcell and superstructure reflexions were obtained for the structure analysis.

Structural determination and refinement

The structure was determined and refined by full-matrix, least-squares methods, using program *LALS* (Gantzel, Sparks & Trueblood, University of California at Los Angeles). Structure factors were weighted according to the precision of the intensity measurements, as deduced from the agreement between the values from the same level obtained for different exposure times. Intensities of the subcell reflexions are not too dif-

ferent from those of the ideal NiAs type structure. Thus, the cell must be made up of three layers of four NiAs units each, stacked normal to the c direction.

Calculations on preliminary trial structures indicated that an ordered vacancy model, analogous to Bertaut's monoclinic structure, would be the appropriate model to develop. The unit-cell content is approximately $Fe_{21}S_{24}$, and corresponds to one Fe vacancy in alternate Fe layers. The proposed model has the space group $P3_1$ (enantiomorphous with $P3_2$) with vacant sites replacing Fe at $0, \frac{1}{2}, 0$; $\frac{1}{2}, \frac{1}{2}, \frac{1}{3}$; $\frac{1}{2}, 0, \frac{2}{3}$. The substructure loses its hexagonal symmetry when adjacent Fe layers become non-equivalent. The highest space group symmetry that this ordered vacancy model can have is $P3_1$; for 'hexagonal' superstructures with $c\neq3nC$, the highest symmetry would be orthorhombic.

The X-ray diffraction pattern of the crystal investigated is hexagonal. Certain groups of subcell and superstructure reflexions (hol, $\bar{h}ol$ with l odd, *etc.*) that should have had unrelated intensities were observed to have equal intensities. The higher diffraction symmetry is attributed to twinning by 180° rotation about c. Such twinning cannot be detected optically, and when polished sections of the grains mounted in Araldite epoxy resin were examined with a polarizing microscope, very few grains appeared in possible twin relationships. However, when examined with an oil immersion lens, parts of the grains within the epoxy showed very pronounced parallel growth development; on etching the polished surfaces with hydriodic acid, lines appeared, that were continuous with the planes defining the parallel growth (Fig. 1). It is postulated that the twin members of the crystals are represented by platy domains, presumably stacked normal to c; also, the lines on the etched surfaces may reflect the differential solution of two domain orientations. It is quite possible that each twin junction is marked by a stacking fault in the close-packed S layers; the etch lines might represent planes of structural weakness introduced by the stacking faults. Buerger (1960) considers a twin junction marked by a stacking fault in a close-packed solid to be coherent, and it is assumed that the twinning in the pyrrhotite under study is also coherent. The stacking interval of the domains along c must be irregular, since diffraction effects referable to regular stacking of such domains are not observed.

The observed structure factor, $F(hkl)$, is, then, an average of $F_o(hkl)$ and $F_o(\bar{h}\bar{k}l)$, which are the quantities required to determine the structure. The least-squares routine was modified so that $F_o(hkl)$ and $F_o(\bar{h}\bar{k}l)$ were calculated from $F(hkl)$ proportional to $F_c(hkl)$ and $F_c(\bar{h}\bar{k}l)$ during each refinement cycle. This provided the best estimate of the observed structure factors and expanded the reflexion list to 317 reflexions. The value of the conventional residual index at this stage was 0·34. Resultant bias in the structure-factor data used and the high pseudosymmetry within the structure made direct refinement of the structure impossible. For
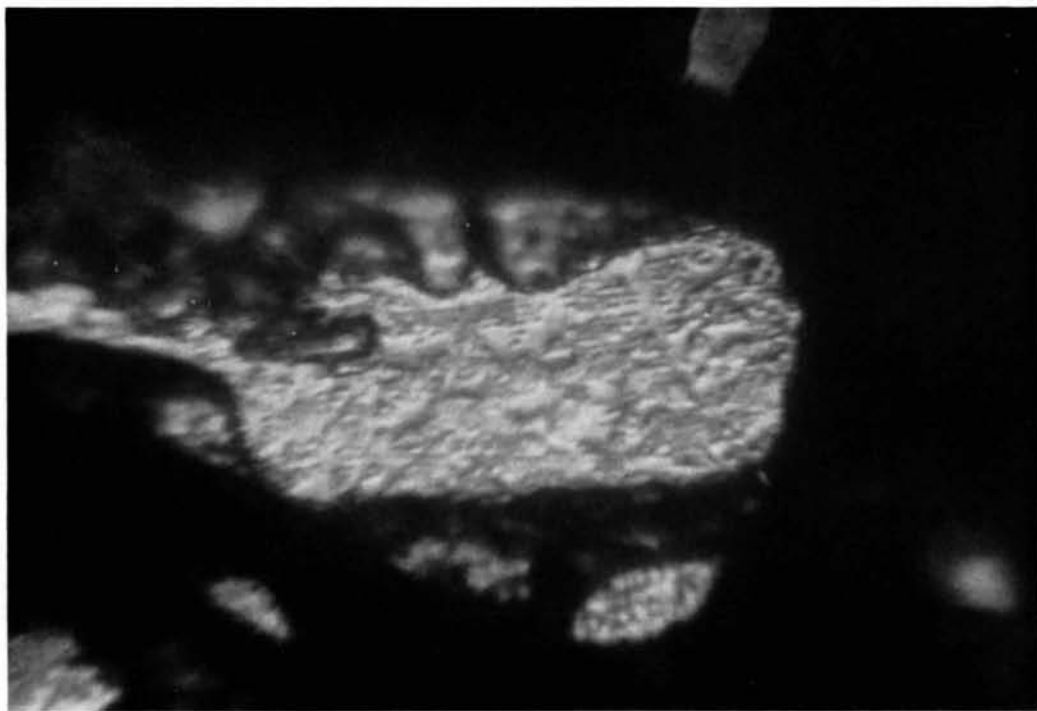
Fig. 1. Photomicrograph of etched, polished surface of a pyrrhotite grain: microscope magnification 1050 × .

this reason, the refinement proceeded in stages on a trial-and-error basis. Each stage was initiated by shifting certain sites arbitrary amounts according to various working hypotheses, constraining other sites and treating the remainder as 'special' positions.

In the structure which finally was accepted, each layer, $c/3$ thick, has a trigonal pseudosymmetry, the ternary axis of which is related to the ternary axis of the unit cell as shown in Fig. 2. Three Fe atoms in each layer are displaced toward an enlarged tetrahedral site formed by vertical displacements of the S atoms in alternate S layers. Displacements of the Fe atoms from the ideal positions are 0·22 Å in both the vacancy layers and full layers.

The value of the conventional residual index for the structure factors used in the refinement (Table 1) was reduced to 0·108; structure factors for unobserved reflexions were not included. Final positional parameters and standard deviations for the refined parameters are given in Table 2; isotropic temperature factors ($B = 8\pi^2\bar{u}^2$) are $0·680 \pm 0·050$ and $0·816 \pm 0·063$ for S and Fe respectively.

It should be emphasized that the twinning operation described above is the least complex one that accounts for the observed diffraction effects. More complex twin operations are possible; indeed, the recognition of stacking faults in the S layers implies rotation of the domains by multiples of 60° about c. However, the net effects of such operations on averaging the scattering contributions from the hkl and $\bar{h}\bar{k}l$ planes would seem to be equivalent to that of the single 180° rotation about c.

Table 1. Observed and calculated structure factors

Table 1 (cont.)

Table 2. Positional parameters with standard deviations in parentheses

	x	y	z
S(1)	0·1667	0·3333	0·0833
S(2)	0·1667	0·8333	0·0833
S(3)	0·6667	0·3333	0·0833
S(4)	0·6667	0·8333	0·0833
S(5)	0·3333	0·1667	0·2512 (05)
S(6)	0·3333	0·6667	0·2512 (05)
S(7)	0·8333	0·6667	0·2512 (05)
S(8)	0·8333	0·1667	0·2349 (12)

Fig. 2. Projection of ⅓ unit of cell of pyrrhotite structure, $z = 0·083$ to $z = 0·417$: large, open circles, S at 0·083 and 0·417; large, ruled circles, S at 0·235; large, stippled circles, S at 0·251; large, broken circle, vacancy at 0·333; small full circles, Fe in 'vacancy' layer; small open circles, Fe in 'full' layer.

$a = 2A$

Table 2 (cont.)

	x	y	z
Fe(1)	0·5	0·5	0·1750 (08)
Fe(2)	0·4708 (10)	0·9855 (05)	0·1587 (05)
Fe(3)	0·0146 (05)	0·9855 (05)	0·1587 (05)
Fe(4)	0·0146 (05)	0·5292 (10)	0·1587 (05)
Fe(5)	0·5328 (09)	0·0164 (04)	0·3273 (05)
Fe(6)	0·9836 (04)	0·0164 (04)	0·3273 (05)
Fe(7)	0·9836 (04)	0·4672 (09)	0·3273 (05)

Discussion

Some interatomic distances of interest are given in Table 3. In the vacancy layers, the Fe atoms are displaced to form planar, triangular groups. The nearest Fe–Fe distance (3·10 Å) within these layers is not too different from the nearest Fe–Fe distance between Fe layers; for Fe(6) these distances are 2·82 and 2·90 Å. In the full Fe layers the planar, triangular Fe groups are slightly less well defined; the nearest Fe–Fe distance is 3·13 Å. Octahedral coordinations of these Fe atoms are greatly distorted from the ideal symmetry.

Table 3. *Some interatomic distances of interest with standard deviations in parentheses*

Fe(2)–S(2)	= 2·219 (07) Å		Fe(5)–S(8)	= 2·383 (15) Å
Fe(2)–S(6)	= 2·471 (08)		Fe(5)–S(3¹)†	= 2·430 (06)
Fe(2)–S(4)	= 2·442 (05)		Fe(5)–S(5)	= 2·458 (07)
Fe(2)–S(8)	= 2·517 (12)		Fe(5)–S(4¹)†	= 2·658 (07)
Fe(3)–Fe(2)	= 3·133 (03)		Fe(6)–Fe(5)	= 3·772 (03)
Fe(2)–Fe(3)	= 3·734 (03)		Fe(5)–Fe(6)	= 3·096 (03)
Fe(6)–Fe(3¹)*	= 2·817 (12)		Fe(6)–Fe(3)	= 2·900 (12)

* $z = 0.4920$
† $z = 0.4166$

Displacements of the Fe atoms in the structure under discussion are analogous to those determined for troilite (Bertaut, 1956), in which all Fe atoms are associated in equivalent planar, triangular groups. Using the more recent positional data of Andresen (1960), which give a greater displacement of the Fe atoms, the nearest Fe–Fe distance within each Fe layer is 2·93 Å; the nearest Fe–Fe distances between Fe layers are 2·98 and 2·94 Å. Although these interatomic distances are large compared to the metallic bond distance of Fe, there is evidence of magnetic coupling between the Fe atoms. It seems that we could expect a weak-bonding interaction between Fe atoms with interatomic distances of about 3·0 Å, and it is this energy contribution that stabilizes the observed structure.

In many ways, the structure of the described pyrrhotite is an 'average' one. There are several details in the crystallography and crystal chemistry of pyrrhotites for which the structure does not give a direct explanation. The 2A, 3C supercell has been observed in compositions as Fe-rich as $Fe_{7.5}S_8$ (Morimoto & Naka-

zawa, 1968). The occurrence of the supercell over the composition range $Fe_{7.5}S_8$ to Fe_7S_8 can be accounted for by the removal of fewer Fe atoms from the vacancy layers, so that the short-range order is retained but long-range disorder is introduced. There is a tendency for the pyrrhotite structure to be intermediate between the NiAs type and the $Cd(OH)_2$ type, as there is with the structures of similar compositions in the Cr–S system (Jellinek, 1957;) it is most probable that all Fe vacancies are confined to the 'vacancy' layers. The non-integral superstructures observed in natural and synthetic superstructures (Morimoto & Nakazawa, 1968; Morimoto, Nakazawa, Nishiguchi & Tokonami, 1970) could be rationalized by developing stacking sequences of the platy domains (or of similar, smaller units) in the c direction, somewhat analogous to the development of antiphase domains in certain alloys. However, additional displacements of the superstructure reflexions in the planes normal to c^* have been observed (Corlett, 1968 and Morimoto & Nakazawa, 1968), which the latter authors referred to a larger supercell with $a = 90A$, $c = 3C$. Similar, but less marked displacements, are apparent in precession photographs of the presently studied crystals. Finally, there has been much discussion of the twinning in the monoclinic supercell (Bertaut, 1953; Wuensch, 1963; Corlett, 1968). Most natural material appears to be twinned, but Corlett reported on an untwinned crystal. As a result of the present study, it seems that for an untwinned crystal many related subcell reflexions of the type $h0l$ and $\bar{h}0l$ with l odd should be noticeably different in intensity.

References

ALSEN, N. (1925). *Geol. Foren. Forhandl.* **47**, 19.
ANDRESEN, A. (1960). *Acta Chem. Scand.* **14**, 919.
BERTAUT, E. F. (1952). *C. R. Acad. Sci. Paris,* **234**, 1295.
BERTAUT, E. F. (1953). *Acta Cryst.* **6**, 557.
BERTAUT, E. F. (1956). *Bull. Soc. franç. Minér. Crist.* **79**, 276.
BUERGER, M. J. (1960). *Cursillos y Conferencias del Instituto 'Lucas Mallada'*, Fasc. **7**, 5.
CORLETT, M. (1968). *Z. Kristallogr.* **126**, 124.
FLEET, M. E. (1968). *Canad. J. Earth Sciences,* **5**, 1183.
FLEET, M. E. & MACRAE, N. (1969). *Canad. Min.* **9**, 699.
JELLINEK, F. (1957). *Acta Cryst.* **10**, 620.
MORIMOTO, N. & NAKAZAWA, H. (1968). *Science,* **161**, 577.
MORIMOTO, N., NAKAZAWA, H., NISHIGUCHI, K. & TOKONAMI, M. (1970). *Science,* **168**, 964.
TOULMIN, P., III & BARTON, P. B. JR (1964). *Geochem. Cosmochim. Acta,* **28**, 641.
WUENSCH, B. J. (1963). *Min. Soc. Amer.* Special Paper 1, p. 157.